Applied Catalysis B: Environmental 160–161 (2014) 629–640

Contents lists available at ScienceDirect

Applied Catalysis B: Environmental

journal homepage: www.elsevier.com/locate/apcatb

Preparation and characterisation of CuO/Al_2O_3 films deposited onto stainless steel microgrids for CO oxidation

Zouhair Boukha, José L. Ayastuy, Ainara Iglesias-González, Beñat Pereda-Ayo, Miguel A. Gutiérrez-Ortiz, Juan R. González-Velasco*

Chemical Technologies for Environmental Sustainability Group, Department of Chemical Engineering, Faculty of Science and Technology, University of The Basque Country UPV/EHU, P.O. Box 644, E-48080 Bilbao, Spain

ARTICLE INFO

Article history:
Received 17 March 2014
Received in revised form 5 June 2014
Accepted 6 June 2014
Available online 13 June 2014

Keywords:
Microreactors
Stainless steel microgrids
Copper species
Alumina
CO oxidation

ABSTRACT

Homogeneous and well-adhered alumina washcoat was deposited onto stainless steel microgrids. Alumina-washcoated stainless steel microgrids loaded with different amounts of copper were synthesised and characterised by several techniques including SEM-EDS, N_2 adsorption at −196 °C, XRD, temperature programmed reduction (H_2-TPR), UV–visible–NIR DRS and XPS spectroscopy. Three types of copper species were detected in the series of the prepared microreactors: (i) CuO deposited on the surface of the substrate; (ii) highly dispersed CuO on the alumina surface and (iii) bulk CuO. As proven by H_2-TPR experiments, the distribution of CuO between these three sites depended on copper loading.

The prepared microreactors were successfully tested in CO oxidation reaction and compared to powder catalysts loaded with the same amount of copper. The results showed that the microstructured catalysts were more active than the powder catalysts when activated under reaction gas mixture. Indeed, a second catalytic run, performed on the same catalyst, revealed a decrease of the light-off temperature in the case of the prepared microreactors as result of their activation. The Cu species distribution seemed to play a decisive role in the activity of the microreactors. The CuO interacting with the substrate seemed to enhance the thermal conductivity of the microreactor and, thus, might better dissipate the heat generated, in the Cu/Al_2O_3 film, by the exothermic CO oxidation reaction. These catalytic features evidenced the potential of these microreactors as a promising alternative catalyst in the CO oxidation reaction.

1. Introduction

The design of new kinds of structured reactors for catalytic applications has attracted much attention in the last decade. According to some experimental studies, the miniaturisation of structured catalysts exhibits important advantages compared to conventional catalysts, thus becoming an interesting candidate to be used in industrial catalytic processes [1,2]. Due to their high surface areas, it was well established that the micro-structured reactors offer high heat/mass transfer coefficients and short contact time of the reactants which results in a better control of the reaction conditions [1,2]. These characteristics are essential for a precise control of temperature and products distribution [3,4]. Additionally, metallic microreactors, compared to ceramic materials, have supplementary advantages such as high thermal conductivity, high mechanical resistance and the possibility to adopt different geometry and configurations [5,6]. Their application in catalytic processes, however, requires the increase of the specific surface area by the deposition of porous outer layer followed by an impregnation of the active phase.

Because of their advantageous catalytic properties alumina-based microstructured catalysts are widely studied and are receiving an increasing attention in the literature [7–14]. The majority of these works used the washcoating technique to deposit alumina support within the microreactors and their main objective was to obtain homogeneous and stable films that would present good adhesion and a high surface area. Moreover, the physico-chemical properties of the catalytic film should not be affected by its deposition on the metallic support. Concerning their catalytic activity, many authors highlighted the high catalytic performances of alumina-based microstructured catalysts when compared to that of the conventional catalysts [7,9,12]. For instance, Peela et al. [7] co-impregnated 2% Rh and 5% Ni on the γ-alumina which previously deposited on stainless steel microchannels by washcoating method. The synthesised microreactors performed satisfactorily in the steam reforming of ethanol and their conversion was higher

* Corresponding author. Tel.: +34 946012681; fax: +34 946013500.
E-mail address: juanra.gonzalezvelasco@ehu.es (J.R. González-Velasco).

http://dx.doi.org/10.1016/j.apcatb.2014.06.002
0926-3373/

than that obtained in a packed bed reactor. They explained this by the longer diffusional path in the powdered catalyst (average size = 200 μm) compared to the washcoat thickness of approximately 65 μm in the microchannels. Stefanescu et al. [9] deposited alumina on microstructured stainless steel platelets and, subsequently, nickel was impregnated as active phase for iso-octane steam reforming reaction. Comparing its performance with that of powdered catalyst, they affirmed that only the microstructured catalyst present the suited heat transfer properties to maximise the catalyst stability and productivity. In their study on the partial oxidation and oxidative steam reforming of propane over Rh/Al_2O_3/Fecralloy microreactor, Aartun et al. [12] concluded that the catalyst dispersed on a porous alumina layer in the microchannels was beneficial and gave higher yield of hydrogen compared to microchannel made from pure rhodium. Furthermore, neither coke formation nor any other form of deactivation of the Rh/Al_2O_3/Fecralloy was observed.

It should be noted that much attention has been also given to searching for new design concepts of the metallic microreactors that can improve the reaction conditions. For example, the metallic grids are known to provide a uniform gas distribution and homogenise the temperature in the reactor by reducing the temperature gradients. These remarkable properties confer to this kind of structure successful application, as microstructured catalysts, in diverse gas phase reactions [15–18]. In their study of copper and nickel grids with the outer surface layer of Raney-type structure for propane oxidation, Yuranov et al. [16] obtained an excellent activity on cobalt oxide supported on a modified Ni-grid. Marban et al. [17] showed that mesoporous Co_3O_4 nanowires supported on a stainless steel microgrid exhibit a good catalytic activity in preferential oxidation of CO compared to unsupported Co_3O_4 particles. Pérez et al. [18] synthesised microreactors based on $CuO\text{-}CeO_2$/zeolite films onto brass microgrids for the oxidation of CO. They reported that these microreactors achieved a higher catalytic performance compared to that of the same catalysts in powder shape and suggested that it was due to the great dispersion of active centres in micro-sized channels. Li et al. [19] have shown that the deposition of the Cu-Fe/ZnO film on stainless steel microgrids provides a promising system for high methanol conversion, hydrogen production rate and durability to produce electrical energy.

On the other hand, the CO oxidation is an exothermic reaction with high environmental interest. The conventional catalysts for CO oxidation reactions generally contain noble metals supported on oxides. Transition metals such as Cu and Co have also been investigated. They are active, less expensive than noble metals but very sensitive to the distribution of the active species [20,21]. For this reason, searching for new materials capable of developing suitable interactions with the loaded metal is essential. The catalytic activity of the Cu/Al_2O_3 catalysts and its correlation with the copper species distribution on the different sites of the carrier has been widely studied. As mentioned by Luo et al. [20] on alumina supported copper catalysts, a good catalytic activity in CO oxidation is related to both the highly dispersed CuO and bulk CuO species. Park et al. [21] observed that the increase in CO oxidation activity was related to the increase in concentration of crystalline CuO. This was explained by the ease of CuO redox behaviour of these species compared to isolated copper surface phase. Huang et al. [22] compared the CO oxidation behaviour over Cu, Cu_2O and CuO bulk catalysts to seek insight the role of the copper species. They found that among the three tested species Cu_2O was the only one that was active at 140 °C. Wan et al. [23] also claimed that, over $CuO/\gamma\text{-}Al_2O_3$ catalysts, dispersed Cu^{1+} species plays a significant role at low temperatures (<200 °C), in CO oxidation reaction.

The present work concerns the preparation, characterisation and activity for CO oxidation reactions of Cu/Al_2O_3 film deposited onto stainless steel microgrids and their comparison with conventional catalytic systems (powder shape). Their characterisation involved BET, SEM, XRD, H_2-TPR, UV-visible-NIR and XPS. Special attention was devoted to the determination of the correlations between the catalysts' activity and the copper species' distribution on the different sites of the microreactors. It should be noted that, to the best of our knowledge, the preparation of this catalytic system configuration, its characterisation and its catalytic activity in CO oxidation reactions have not been yet investigated. The analysis of the very rich information provided from all the above-mentioned studies has allowed us to conclude that the microreactors based on Cu dispersed onto alumina film adhered on stainless steel microgrids constitute an interesting family of catalysts whose catalytic properties could be modulated by modifying the copper loading.

2. Experimental

2.1. Preparation of the catalysts

2.1.1. Washcoating of SS316 microgrids (MG)

Several methods have been used for the washcoating of alumina on ceramic and metallic monoliths. In the present study the deposition of alumina film was carried out using a modified version of the methods mentioned in the literature [7,14,24–27]. The average particle size of the alumina (SA 6173, Saint-Gobain), previously calcined at 850 °C, was reduced to less than 3 μm by wet milling in a ball mill for 72 h. Meille et al. [27] reported that the pre-calcination of alumina may eliminate the surface hydroxyl groups, preventing the formation of chemical bonds between particles (like the formation of a gel). Furthermore, in order to improve its rheological properties, the alumina milled slurry was mixed with polyvinyl alcohol (PVA: Aldrich) and colloidal alumina (Alfa Aesar, 0.05 μm), used as binders, and stirred for 2 h [7,26]. The pH was adjusted to the desired value (3.5–4) by adding HNO_3 or NH_3. The final slurry composition (in weight) was: 10.6% alumina, 1% PVA, 3.4% colloidal alumina and remaining water. This composition had a viscosity of around 10 mPa s at a shear rate of 500 s^{-1}.

Prior to any manipulation, the stainless steel microgrids (MG: AISI 316, wire: 100 μm and space: 150 μm), previously cleaned with water and acetone in an ultrasonic bath to eliminate surface contamination, were calcined at 900 °C for 4 h. This treatment was seen to improve the surface rugosity of the stainless steel alloys and lead to a good adhesion of the deposited film [14]. The calcined MG were dipped in the prepared alumina slurry for 10 min and the excess slurry was evacuated by a flow of compressed air. The samples were dried at 120 °C for 30 min and the procedure was repeated eight times before their calcinations at 600 °C in static air for 5 h with a temperature ramp of 1 °C min^{-1}. The obtained samples were labelled Al-MG.

2.1.2. The Cu impregnation of alumina-coated microreactor

For the impregnation of the active phase (Cu) the alumina-washcoated MG substrates were dipped into a stirred aqueous solution of 0.8 M $Cu(NO_3)_2{\cdot}3H_2O$ (Panreac) for 2 h. Then, the samples were dried at room temperature for 2 h and at 120 °C for 2 h. This sequence was repeated two and three times to obtain three catalysts with different Cu loadings (Table 2). Finally, the resulted microstructured reactors with different Cu/Al molar ratios, labelled CuAl-MG1, CuAl-MG2 and CuAl-MG3, were calcined at 600 °C for 10 h with a temperature ramp of 1 °C min^{-1}.

In order to be used as reference, the sample labelled Cu-MG was prepared by deposition of active metallic phase (Cu) on unwashcoated MG. The MG substrate was dipped into a stirred aqueous solution of 0.8 M $Cu(NO_3)_2{\cdot}3H_2O$ for 2 h, dried (2 h at RT followed

by 2 h at 120 °C) and calcined at 600 °C for 10 h. The amount of copper in the prepared catalysts was determined by ICP-AES.

2.1.3. The Cu impregnation of the powder alumina

The catalysts denoted as CuAl-P1, CuAl-P2 and CuAl-P3 were prepared by impregnating a given mass of the alumina with aqueous solution of $Cu(NO_3)_2{\cdot}3H_2O$ containing three different Cu amounts to reach desired Cu/Al molar ratios (equivalent to that obtained on the microreactors) and the solution excess was evaporated in a rotary evaporator at 50 °C. The resulted samples were dried at 120 °C and calcined at 600 °C for 10 h.

2.2. Characterisation techniques

The alumina slurry was characterised by measuring the particle size by laser scattering with a MasterSizer analyzer X v1.1. (Malvern), and the viscosity was determined with a Rheomat R180 instrument (Mettler Toledo). The physical stability of the obtained washcoats was assessed by the so-called adherence test. This was based on determining the weight loss of the coated microreactor, immersed in water, after a specific time (1 h) in an ultrasound bath.

The volumetric N_2 adsorption at −196 °C was performed on an automatic apparatus Micromeritics, model TRISTAR II 3020 apparatus. The pre-treatments applied to the samples consisted of a cleaning, at 300 °C (overnight), under nitrogen flow. The specific areas of the samples were determined in line with the standard BET procedure, using nitrogen adsorption taken in the relative equilibrium pressure interval of 0.03–0.3.

The morphologies of the prepared samples were observed using a JEOL JSM-7000F scanning electron microscope (SEM) equipped with a Schottky field emission gun (FEG) combined with energy dispersive X-ray microanalysis (EDS). Secondary electron images were taken at 20 kV and a current intensity of 1.1×10^{-10} A was employed using a working distance of 10 mm. To provide electrical conductivity the samples were coated with a coal graphite layer (10 nm) by evaporation using Quorum Q150 T Sputter Coater.

X-ray diffraction (XRD) studies were conducted on a X'PERT-MPD X-ray diffractometer with Cu Kα radiation (λ = 1.5406 Å) and Ni filter. The X-ray tube was operated at 40 kV and 40 mA. The samples were scanned between 10° and 100° (2θ), and the X-ray diffraction line positions were determined with a step size of 0.01° and a counting time of 2.5 s per step. Phase identification was conducted by comparison with JCPDS database cards. The oxidation states and the coordination of Cu species were evaluated by diffuse reflectance UV-vis spectroscopy (UV-visible-NIR DRS) with a UV-vis-NIR Cary 5000 apparatus coupled to Diffuse Reflectance Internal 2500 within a range of 200–2500 nm.

Redox behaviour was examined by temperature-programmed reduction (H_2-TPR) on a Micromeritics AutoChem 2920 instrument. Firstly, all the samples were pre-treated in an oxygen stream (5%O_2/He) at 400 °C for 1 h and then cooled to room temperature. The reducing gas used in all experiments was 5%H_2/Ar, with a flow rate of 50 $cm^3\ min^{-1}$. The temperature range explored was from room temperature to 400 °C, with a heating rate of 10 °C min^{-1}. This temperature was maintained for 1 h. The water produced by reduction was trapped in a cold trap, and the consumption of H_2 was quantitatively measured by time integration of the TPR profiles.

The copper dispersion and metal area on the prepared catalysts were estimated by the passivation method using N_2O [28,29]. The sample previously reduced at 400 °C was cooled (under He flow) to the temperature for the N_2O-reaction (60 °C), and finally submitted during 1 h under 20%N_2O/He flow (50 $cm^3\ min^{-1}$), also at 60 °C. The Cu_2O surface formed was further reduced with 5%H_2/Ar at 400 °C following the H_2 consumption with a Micromeritics AutoChem 2920 instrument. The metallic surface area was also calculated assuming that reduced copper surface had a surface density of 1.46×10^{19} copper atoms/m^2.

XPS measurements were performed with a Phoibos 150 1D-DLD analysis system from Specs, with monochromatic Al Kα radiation (1486.6 eV). The hemispheric photoelectron analyser worked with a pass energy of 40 eV for survey scan and 20 eV for detail scan. In order to compare all spectra recorded, the C 1s core level attributed to adventitious carbon present in the samples was used as a reference, whose binding energy was fixed at 284.6 eV. Peaks areas of Cu^{2+} including satellites were fitted with a non-linear least squares fitting programme using a properly weighted sum of Lorentzian and Gaussian component curves after background subtraction according to Shirley.

2.3. Catalytic tests

The CO oxidation catalytic tests were performed, with flow/mass ratio of 660 ml $min^{-1}\ g^{-1}$, in a tubular flow reactor operating at atmospheric pressure using 150 mg of the catalyst (both for powders and microgrids reactors). The mass of the microstructured catalyst was referred to the Cu/Al_2O_3 film weight. The powder catalyst bed was diluted with inert quartz to achieve the same volume occupied by the microreactors (cylinder of 18 mm height and 9 mm diameter). To prevent a bypass flow the microreactor was rolled around a small stainless steel cylinder, following the same configuration reported in the literature [17,18]. Prior to running the catalytic experiments, the catalysts were submitted to a pre-treatment routine consisting of their heating at 360 °C (1 h), in a flow 20%O_2/He, followed by 1 h at 360 °C. The mixture was composed of 2% CO and 2% O_2 diluted in He and a total flow rate equal to 100 $cm^3\ min^{-1}$. The temperature of the reaction was increased from room temperature up to 360 °C with a heating rate of 5 °C min^{-1}. The reaction products were continuously analysed by mass spectrometer (MKS, Cirrus 3000) which was calibrated using different mixtures of CO and CO_2.

Turn over frequency (TOF) value was calculated, at 185 °C, as the activity data per mole of copper (n_{Cu}), according to the following equation:

$$\mathrm{TOF}\,(s^{-1}) = \frac{F_{CO}^{in} \cdot X_{CO}}{n_{Cu}}$$

where X_{CO} is the CO conversion and F_{CO}^{in} is the inlet CO molar flow.

3. Results and discussion

3.1. Performance evaluation of the coating

Fig. 1 shows the weight increases expressed as alumina deposited density (alumina mass/substrate surface area) versus the number of the immersions in the prepared slurry. As expected, the obtained results showed that the deposition density increased linearly with the number of immersions. After eight immersions the sample reached a deposition density of 1.65 $mg_{(alumina)}\ cm^{-2}{}_{(MG)}$ (Fig. 1). After the subsequent calcinations of the sample (after 8 immersions), at 600 °C, about 6 wt.% alumina (1.3 $mg_{(alumina)}\ cm^{-2}{}_{(MG)}$) was deposited on the substrates. Additionally, a good adherence of the deposited film was evidenced by ultrasonic tests for 1 h (wt. loss < 0.5%).

Table 2 presents the amount of deposited Cu and the Cu/Al atomic ratios, referred to the mass of alumina washcoat. Note that the increase of immersion time (in the copper salt solution) from 2 h to 6 h increased the amount of deposited Cu. For instance, 8.4 wt.% Cu was obtained on the CuAl-MG1 sample after immersion during 2 h while the CuAl-MG3 sample, prepared through 3 successive

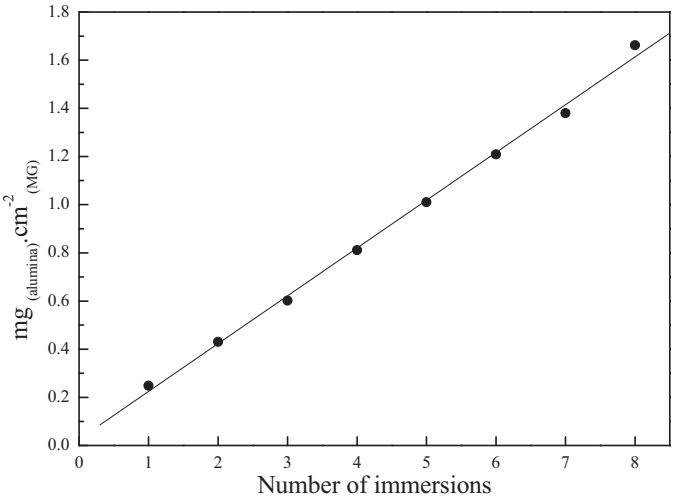

Fig. 1. Incorporation of alumina to the MG microreactor versus the number of immersions (Viscosity: 10 mPa s).

immersions for 2 h each (with drying steps in between), reached a 14.6 wt.% Cu.

3.2. Scanning electron microscopy (SEM)

The substrates unwashcoated and washcoated were investigated by scanning electron microscopy in order to visualise the textural modifications introduced by the deposition of the alumina film (Fig. 2). Table 1 summarises the localised elemental compositions taken, by means of EDS, at three different zones on the CuAl-MG1 microreactor.

To visualise the morphological aspect of the un-pretreated stainless steel microgrids, micrographs of frontal views of the samples are presented in Fig. 2(a) which showed a very low rugosity in its surface. However, the pictures reported in Fig. 2(b) clearly illustrated the radical surface changes that occurred under the pretreatment process of the MG substrates. Indeed, the calcination of the microgrids at 900 °C for 4 h generated a surface thin film (1 μm) consisting of crystallites that increased their apparent rugosity (Fig. 2(b)). Moreover, as shown in Table 1, semi-quantitative elemental analysis of the interface zone (B) confirmed the diffusion of Cr from the substrate through the surface thin film. Indeed, the Cr weight percentage increased notably from 11% in the bulk substrate (zone A) to reach 39% on the surface (zone B). The occurrence of the thin film on the surface of heat treated 316 stainless steel material was also reported by Sun et al. [30] where they claimed that it may be formed by diffusion of chromium from the bulk material through the oxide layer. The structural nature of these crystallites will be discussed in the XRD section. SEM images of the CuAl-MG1 microreactor showed that the preparation method used in this work for the synthesis of Cu/Al_2O_3 films onto stainless steel microgrids resulted in homogeneous and stable coatings with an estimated thickness of 10 μm (Fig. 2(c)). Microanalysis (EDS) of the washcoat showed that the copper was homogeneously distributed on the internal, external and middle zone of the film.

Table 1
EDS elemental microanalysis of CuAl-MG1 microreactor (zones identified in Fig. 2c).

	Fe (wt.%)	Cr (wt.%)	Al (wt.%)	Cu (wt.%)
Zone A	74	11	0	1.5
Zone B	17	39	3.3	1.6
Zone C	0.6	1.0	55	5

3.3. Textural characterisation studies

The N_2 adsorption isotherms for CuAl-MG and CuAl-P catalysts (not shown) and the data reported in Table 2 showed that the isotherms were characteristic of mesoporous materials exhibiting IV-type according to the IUPAC classification. The pore size distribution of the alumina support showed that it was composed of a rather and narrow unimodal distribution centered at approximately 10 nm (Fig. 3). This distribution did not change when the alumina was deposited onto the stainless steel microgrid. Furthermore, in comparison with alumina powder sample, when the BET surface area of the Al-MG microreactors was referred to 1 g of washcoated Al_2O_3 we concluded that the deposition of alumina onto stainless steel microgrids did not significantly affect its specific surface area (123 $m^2\ g^{-1}$ for Al_2O_3 and 122 $m^2\ g^{-1}$ for Al-MG). Likewise, a very slight decrease in the specific surface area was noticed on the CuAl-MG1 sample (119 $m^2\ g^{-1}$) compared to the Al-MG catalyst (Table 2). Regarding the effect of the copper loading on the textural properties of the CuAl-MG samples, a smooth decrease of the BET surface area, from 119 $m^2\ g^{-1}$ for CuAl-MG1 to 109 $m^2\ g^{-1}$ for CuAl-MG3 was found. It should be noted that the impregnation of copper did not modify the mesopore size distribution of the alumina-washcoated microreactor (Fig. 3). However, the CuAl-P powder catalysts, used as reference, exhibited a bimodal pore size distribution centred at approximately 9 and 15 nm (Fig. 3). The differences, in pore size distribution, between CuAl-MG and CuAl-P samples resulted from the preparation method used for the impregnation of the copper. The average pore size of CuAl-P catalyst has probably increased due to collapse of small pores of alumina support during impregnation step. In the case of CuAl-MG samples the incorporation of copper was carried out by simple immersion which did not modify their pore size distribution.

3.4. X-ray diffraction (XRD)

The CuAl-MG and CuAl-P samples were characterised by means of X-ray powder diffraction in order to investigate their structural properties. Fig. 4 compares the diffractograms of the prepared catalysts after calcinations at 600 °C. The diffractogram of alumina and MG samples were also presented as references.

X-ray diffraction pattern of as-received MG microgrids (Fig. 4) showed that the solid structure was essentially a γ-austenite crystalline phase [31]. By contrast, the diffractogram for the MG sample calcined at 900 °C (Fig. 4), showed remarkable differences with respect to that of as-received MG. New diffraction peaks, assignable to a α′-martensite crystalline phase, could be clearly observed. The occurrence of this phase was in good agreement with a number of earlier studies, in accordance with which, the heat treatment of SS316 stainless steel alloys may lead to the transformation of the γ-austenite to the α′-martensite phase [31]. Furthermore, the diffractogram for the calcined MG sample displayed additional weak diffraction peaks attributed to Cr_2O_3 phase (JCPDS file #38-1479). In correlation with the SEM results, it was clear that the observed crystallites formed after calcinations of the MG sample at 900 °C, could be related to the structural changes detected by XRD and specially the formation of Cr_2O_3 phase.

The XRD patterns of the alumina support calcined at 850 °C showed a typical diffractogram for transition alumina (Fig. 4). Furthermore, despite its deposition onto stainless steel microgrids, the structural characteristics of the alumina remained unchanged.

After copper impregnation, on both CuAl-MG and CuAl-P powder catalysts (Fig. 4), two prominent typical peaks belonging to CuO appeared at $2\theta = 35.5°$ and 38.5° (JCPDS card no: 45–0937). Their intensity increased with copper loading. It should be noted that no diffraction peaks assigned to $CuAl_2O_4$ (spinel structure) were detected in all the XRD patterns. This observation was in good

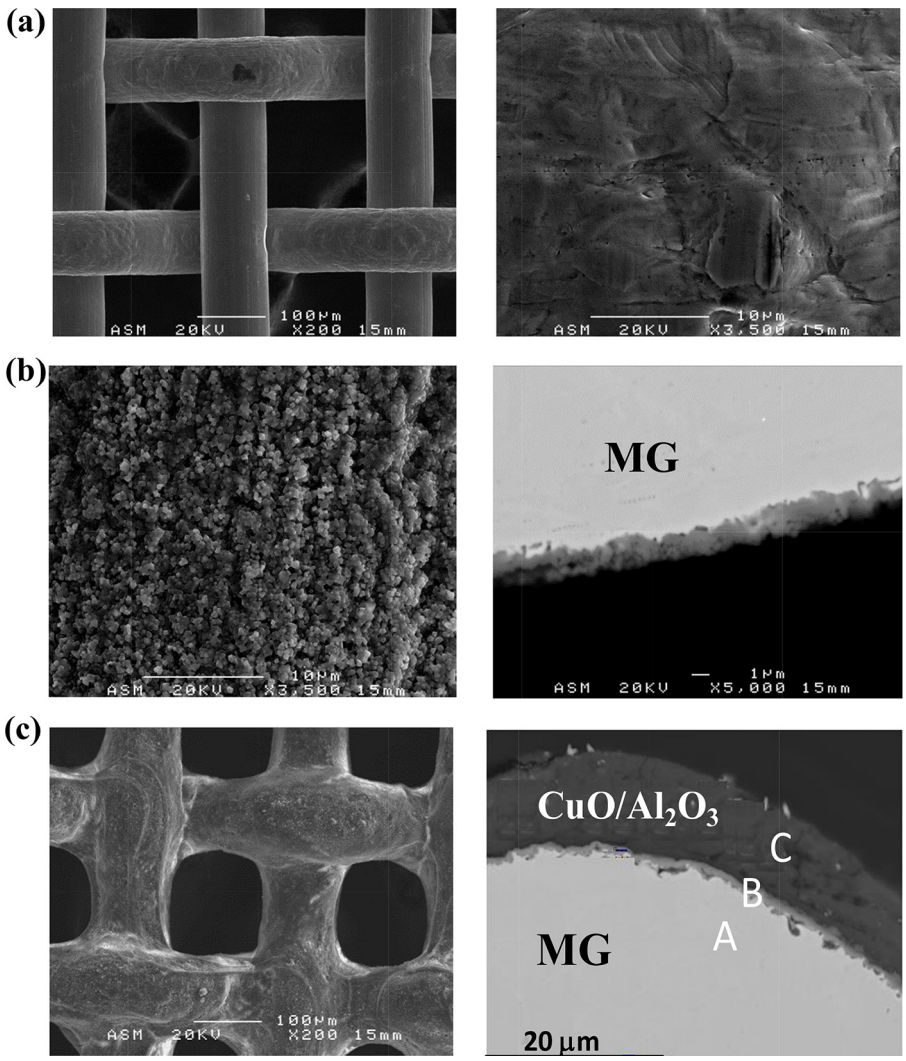

Fig. 2. SEM micrographs of (a) Fresh MG, (b) MG calcined at 900 °C and (c) Cu/alumina film synthesised onto MG (CuAl-MG1).

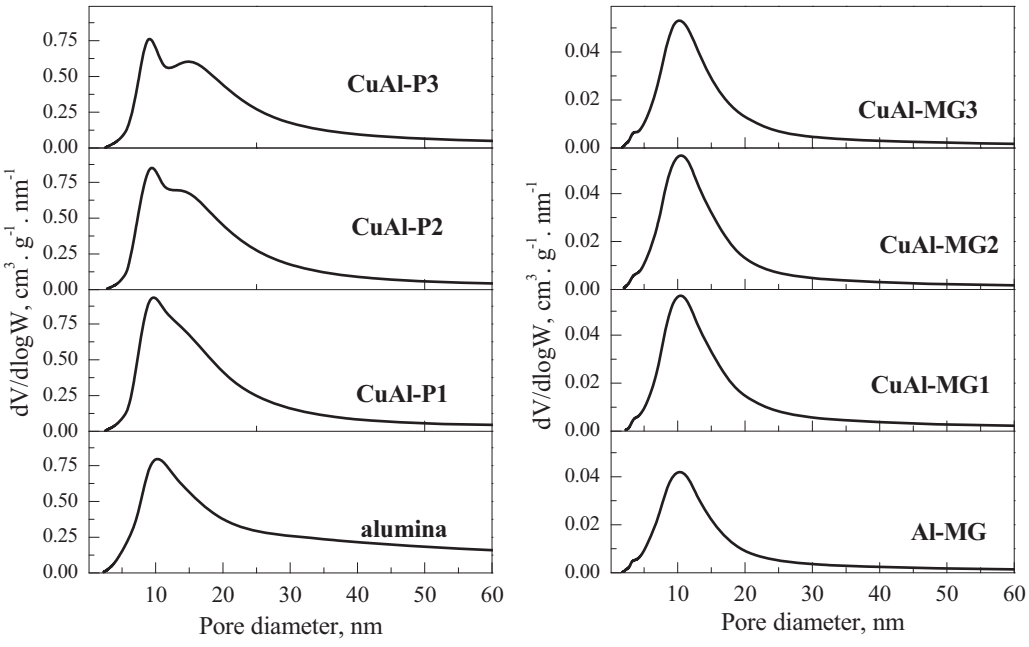

Fig. 3. Mesoporous size distribution for the prepared catalysts (as determined from the BJH analysis of the corresponding N_2 adsorption isotherms at −196 °C).

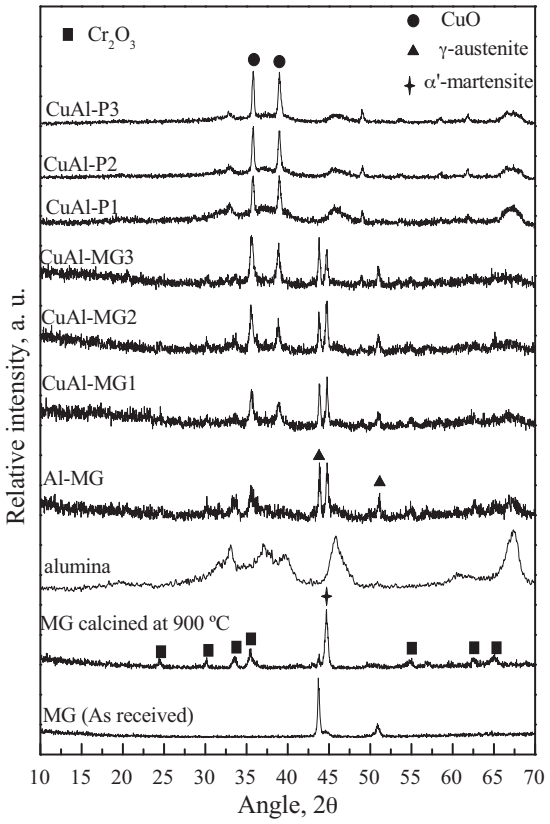

Fig. 4. XRD patterns of the prepared catalysts.

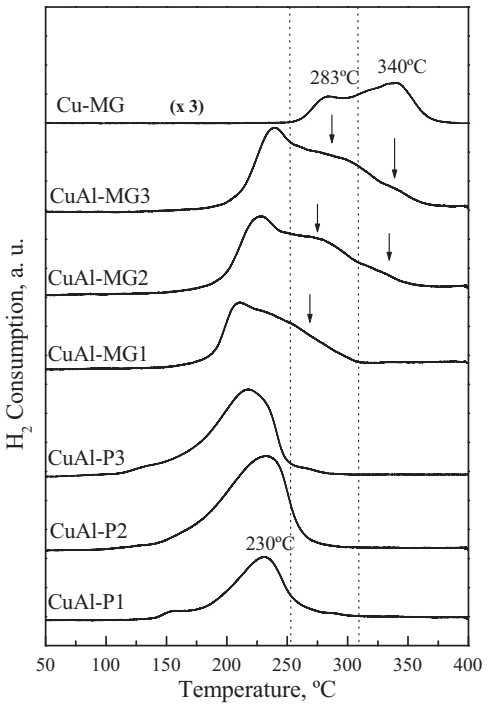

Fig. 5. H_2-TPR profiles of the CuAl-P and the CuAl-MG catalysts.

agreement with a number of earlier studies, in accordance with which, the calcinations of alumina supported copper catalysts up to 600 °C does not lead to the formation of the spinel structure [20,21].

3.5. Temperature programmed reduction (H_2-TPR)

H_2-TPR experiments were carried out in order to investigate the reducibility of the copper species and their metal–support interactions. In addition, this technique could help identify the copper phases present in each catalyst. In principle, a lower reduction temperature would be expected for highly dispersed cooper species [20].

Fig. 5 displays the H_2-TPR profiles of CuAl-MG and CuAl-P catalysts. The attribution of the reduction peaks was carried out by comparison with bulk CuO (not shown) and copper supported on the MG substrate (Fig. 5) used as reference. The H_2-TPR profiles of the CuAl-P1, CuAl-P2 and CuAl-P3 powder catalysts (Fig. 5) were characterised by the presence of a major reduction peak centred at temperatures ranged between 220 and 230 °C attributed to highly dispersed CuO on alumina surface [20,32]. The latter was accompanied by a second, much less intense, feature at 250-280 °C attributed to the reduction of the bulk CuO. The temperature reduction of the bulk CuO, at around 250–280 °C, was confirmed by the H_2-TPR analysis of physical mixture of the bulk CuO with alumina (not shown). It should be noted that the H_2-TPR profiles for CuAl-P showed a third peak, in the 130–150 °C range temperature, being due to a reduction of a small fraction of Cu_2O species occurring at the alumina surface [33].

The H_2-TPR trace for the Cu-MG sample (Fig. 5) consisted of a major reduction peak at approximately 340 °C, which characterise the reduction of the fraction of CuO interacting with the substrate, accompanied by a second less intense feature at 283 °C due to the reduction of bulk CuO.

The H_2-TPR spectrum of the CuAl-MG catalysts was characterised by two reduction peaks, appearing at about 200 and 260 °C, ascribable to the reduction of highly dispersed CuO particles on the alumina [20] and to the reduction of the bulk CuO, respectively. This was also confirmed by the comparison of the H_2-TPR profile with the profile of the Cu-MG sample (Fig. 5). In contrast to the CuAl-P powder catalysts, generally, the increase of Cu loading in CuAl-MG microstructured catalysts shifted the reduction peaks

Table 2
Textural parameters and chemical analyses characterising the investigated samples.

Sample	Cu/Al[a]	Cu (wt.%)	S_{BET} ($m^2\ g^{-1}$)	Pore volume ($cm^3\ g^{-1}$)	Mean pore diameter (nm)
MG calcined at 900 °C	–	–	0.31	0.000381	2.6
Alumina	–	–	123	0.500	13.5
Al-MG	–	–	7.3 (122)[b]	0.019 (0.40)[b]	11.2
CuAl-MG1	0.07[b]	08.4[b]	8.0 (119)[b]	0.025 (0.37)[b]	12.3
CuAl-MG2	0.16[b]	11.5[b]	8.0 (114)[b]	0.025 (0.36)[b]	11.6
CuAl-MG3	0.20[b]	14.6[b]	8.0 (109)[b]	0.024 (0.33)[b]	11.4
CuAl-P1	0.08	08.5	118	0.46	15.0
CuAl-P2	0.18	11.6	110	0.44	15.1
CuAl-P3	0.21	14.8	105	0.41	15.1

[a] Atomic ratio.
[b] Referred to the washcoat weight.

Table 3
Quantitative TPR results obtained on the CuAl-MG and CuAL-P catalysts.

	H_2-TPR data			H_2-TPR after passivation with N_2O		
	Theoretical H_2 uptake (mmol g^{-1})	Experimental H_2 uptake (mmol g^{-1})	Cu species (mmol g^{-1})	H_2 uptake (mmol g^{-1})	Cu dispersion (%)	Specific Cu surface area (m^2 g^{-1})
Cu-MG	0.3	0.31	0.1[b] 0.2[c]	–	–	–
CuAl-MG1	1.3*	1.5*	0.3[a] 1.2[b]	0.50*	76.0	41.7*
CuAl-MG2	1.8*	2.2*	0.8[a] 1.2[b] 0.2[c]	0.52*	56.2	42.9*
CuAl-MG3	2.3*	2.5*	0.4[a] 1.3[b] 0.8[c]	0.42*	36.5	34.6*
CuAl-P1	1.3	1.2	1.05[a] 0.06[b] 0.09[d]	0.29	44.1	24.0
CuAl-P2	1.8	2.1	1.92[a] 0.07[b] 0.11[d]	0.25	27.2	20.3
CuAl-P3	2.3	2.3	2.14[a] 0.10[b] 0.16[d]	0.15	13.0	12.5

(*) Referred to the washcoat weight.
[a] CuO in strong interaction with the alumina.
[b] Bulk CuO.
[c] CuO deposited on the MG substrate surface.
[d] Cu_2O species.

toward higher temperatures (Fig. 5). Furthermore, at high Cu loadings (CuAl-MG2 and CuAl-MG3 samples) the typical peak belonging to the CuO interacting with the stainless steel substrate appeared at 340 °C and its intensity increased with copper loading.

Table 3 compiles the quantitative data resulting from the H_2-TPR diagrams of CuAl-MG and CuAl-P catalysts as well as the calculated copper dispersion, following the procedure described above. The relative abundance of the reducible copper species, calculated on the basis of the H_2 consumed in each reduction peak showed that the distribution of the Cu species between the three sites, detected in the CuAl-MG catalysts, seemed to depend on Cu content (Table 3). The amount of CuO deposited on the substrate surface increased from 0.2 to 0.8 mol g^{-1} while passing from 14 to 18% of loaded CuO. However, the fraction of the bulk CuO stayed almost constant (1.2–1.3 mmol g^{-1}) for the three examined microstructured catalysts, suggesting that this was the needed value, corresponding to the amount of the bulk CuO, to saturate the alumina film. In the case of the CuAl-P catalysts, the contribution of bulk CuO was significantly lower than that determined for the CuAl-MG samples (Table 3). Furthermore, the amount of Cu_2O species seemed to increase with copper loading and reached 0.16 mmol g^{-1} on CuAl-P3 catalyst.

The sixth, seventh and eighth columns in Table 3 summarise the quantitative data resulting from the N_2O passivation/TPR method used for the estimation of Cu dispersion and the corresponding specific copper surface area. The obtained data showed that the incorporated copper species were well dispersed in the microstructured catalysts. Indeed, the Cu dispersion varied between 36 and 76% on the CuAl-MG microstructured catalysts whereas it was ranging between 13 and 44% on the CuAl-P powder catalysts (Table 3). Likewise, the assessed surface area of copper for the analysed samples (Table 3) showed that it decreased with the increase of the copper content on the two series of the catalysts. However, the CuAl-MG microstructured catalysts bore a large metallic surface area (34.6–41.7 m^2 g^{-1}) compared to the CuAl-P powdered catalysts (12.5–24 m^2 g^{-1}). This allowed us to conclude that the large fraction of copper atoms which were exposed at the surface of the microstructured catalysts and accessible to reactant might constitute an advantage since it could be available for catalysis.

These results were consistent with that of Pérez et al. [18] when they claimed that on the Cu/zeolite films synthesised onto brass microgrids the active centers had a very good dispersion compared to their counterpart in powder shape.

3.6. UV-visible-NIR diffuse reflectance spectroscopy (DRS)

Diffuse reflectance spectroscopy was used to study the symmetry and the coordination of copper species dispersed on alumina support and Al-MG microstructured reactor. The Cu^{2+} ions in octahedral (Oh) surrounding exhibit a simple spectrum that involves d–d transitions appearing in the visible domain. These [$^2B_{1g}(^2E_g) \rightarrow {}^2B_{2g}(^2T_{2g})$, $^2E_g(^2T_{2g})$] transitions are usually located around 600–900 nm [34,35]. In tetrahedral (Td) sites Cu^{2+} electronic transitions [$^2B_2(^2T_2) \rightarrow {}^2A_1(^2E)$, $^2B_1(^2E)$] display absorption band, in NIR domain, between 1300 and 1600 nm [34,35].

The UV-vis-NIR spectra of the prepared catalysts were presented in Fig. 6. The attribution of the obtained absorption bands was carried out by comparison with a spectrum of bulk CuO prepared by the decomposition of copper nitrates at 600 °C and used as reference.

The shape of the CuAl-P spectra, samples calcined at 600 °C, look similar (Fig. 6). In the UV-visible region, the spectra showed bands around 230 and 600–800 nm. The band centered at 230 nm was attributed to $O^{2-} \rightarrow Cu^{2+}$ charge transfers. This band seemed to decrease with the Cu concentration. A similar band was detected in the UV-visible spectra of various Cu-Al systems and multiple assignments have been given to describe its origin [36,37]. For example, Bravo-Suárez et al. [36] in their CuMgAlOx investigated materials spectra; they attributed this band to highly dispersed (isolated) Cu^{2+}–O^{2-} in octahedral coordination.

In the visible domain, the bands located at 600–800 nm regions are due to d–d transitions of Cu^{2+} ions in an octahedral or pseudo-octahedral symmetry. The broad band appearing in the NIR at

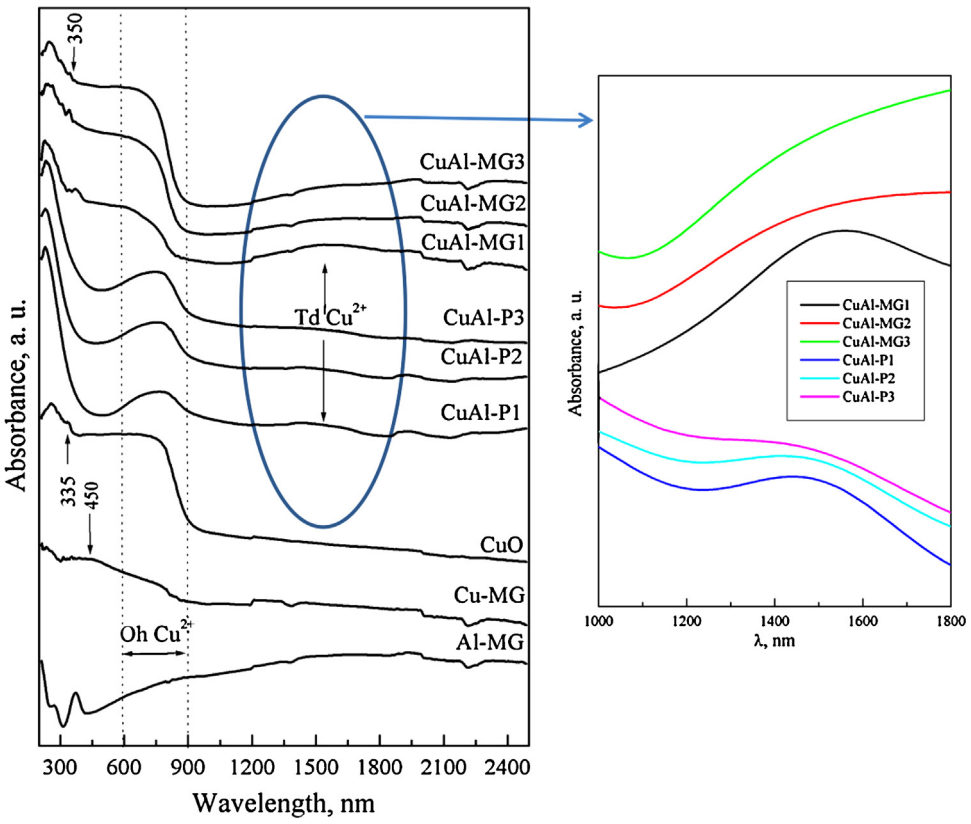

Fig. 6. UV-VIS-NIR spectra of the CuAl-P and the CuAl-MG catalysts.

1500 nm, was attributed to the transition of Cu^{2+} occupying tetrahedral coordination. The increase of Cu concentration broadened the band indicating that there existed formation of CuO on the surface of the alumina.

Fig. 6 also shows the UV-visible-NIR spectra of CuAl-MG microreactors. As previously discussed, these catalysts also showed spectra with bands in the higher (1500 nm) and lower (600–800 nm) wavelength regions, consistent with both octahedral and tetrahedral coordination of cupric ions. The intensity of the bands attributed to octahedral coordination progressively increased with the addition of copper. However, the general shape, including the absorption edge of the bands, appeared significantly different compared to the series of CuAl-P catalysts. In fact, the positions of the bands attributed to octahedral coordination situated at 600–800 nm were blueshifted. Furthermore, in comparison with the spectra of CuAl-P catalysts, the spectra of the CuAl-MG microstructured catalysts showed additional bands in the UV-Visible regions around 350 and 450 nm. The presence of the latter was evidenced by the presence of a plateau of the absorption between 350 and 600 nm. Iwamoto et al. [38] observed analogous bands (centred at 350 and 450 nm) and ascribed them to Cu^{2+}-O^{2-}-Cu^{2+} charge transfers. Since these two bands were also detected in the spectrum of bulk CuO (Fig. 6), used as reference, their presence in the microstructured catalysts spectra, as expected, evidenced the presence of large amount of the bulk CuO. These results were in good agreement with the data of H_2-TPR analysis.

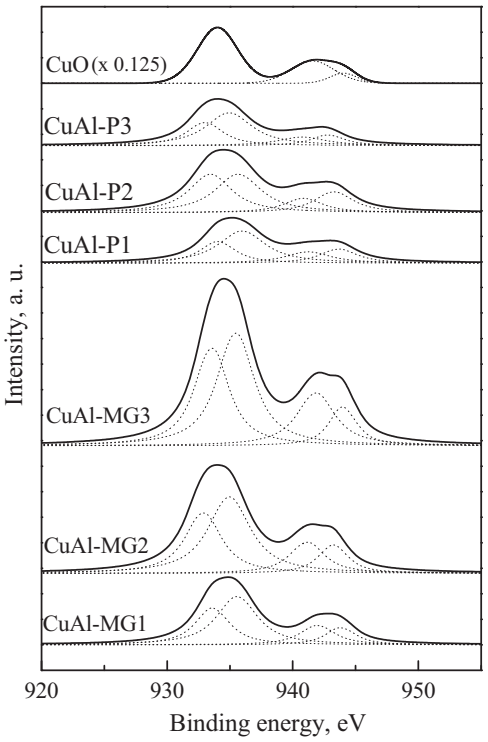

Fig. 7. XPS spectra of Cu $2p_{3/2}$ region of the CuAl-P and the CuAl-MG catalysts.

3.7. X-ray photoelectron spectroscopy (XPS)

The surface chemical composition and the distribution of copper species laying on the surface of the prepared CuAl-MG and CuAl-P catalysts were investigated by means of XPS measurements. Data obtained from the analysis of the corresponding Cu $2p_{3/2}$ spectra are summarised in Table 4 and Fig. 7. Likewise, the Cu $2p_{3/2}$ spectrum of bulk CuO was displayed in order to be used as reference. The examined samples did not show any peak at energy values lower than 933 eV because they were exposed to oxidising atmosphere

Table 4
XPS study of the CuAl-MG and CuAl-P samples. Bulk CuO was also investigated as reference material.

Sample	Cu/Al ICP	Cu/Al (XPS)	Cu^{2+} ($2p_{3/2}$)	FWHM	Auger parameter[a]	Cu $2p_{3/2}$ satellites	Satellite intensity[b]
CuO	–	–	933.6	3.8	1851.6	941.6 (7.6)[c] 944.0 (10.0)	0.55
CuAl-MG1	0.07	0.13	934.7	5.0	1849.4	941.8 (7.1) 943.6 (9.1)	0.46
CuAl-MG2	0.16	0.31	934.0	5.3	1850.2	941.2 (7.2) 943.5 (9.5)	0.43
CuAl-MG3	0.20	0.54	934.6	4.9	1850.9	941.7 (7.1) 944.3 (9.7)	0.46
CuAl-P1	0.08	0.07	935.1	5.0	1850.2	941.1 (6.0) 943.9 (8.8)	0.56
CuAl-P2	0.18	0.09	934.5	5.7	1851.2	941.0 (6.5) 943.6 (9.1)	0.44
CuAl-P3	0.21	0.08	934.2	6.3	1848.7	941.1 (6.9) 943.0 (8.8)	0.34

[a] Calculated as the sum of copper 2p Binding Energy and Auger Kinetic Energy.
[b] Cu $2p_{3/2}$ satellite intensity relative to main photoelectron line.
[c] Values in parentheses are ΔE $2p_{3/2}$ = main peak – satellite peak.

and did not contain metallic copper (Fig. 7). However, the profiles of all the samples were consistent with the presence of Cu^{2+} species characterised by binding energy values higher than 933 eV [39]. Furthermore, the Auger parameter values of all the catalysts, except in the case of the CuAl-P3 catalyst, were in the 1849.4–1851.6 eV binding energy range confirming the presence of Cu(II) cations [40]. Espinos et al. [40] attributed the variation of the Auger parameter values by the presence of the metal in different coordination. This was the case of our CuAl-MG and CuAl-P samples, since it was observed on their UV-Visible-NIR spectra the presence of the copper in both tetrahedral and octahedral coordination. The spectra of CuAl-MG and CuAl-P catalysts also exhibited typical shake-up satellite peak at high binding energies. The satellite intensity to main photoelectron line ratios, calculated for all the analysed samples, was found to be around the experimental error of that for CuO (0.55) (Table 4). This result was not surprising since the CuO phase was detected by XRD on all the samples. On the basis of its observed apparent asymmetry the shake-up satellite peak of Cu $p_{3/2}$ spectra of the catalysts was deconvoluted. The latter tended, in all the cases, to split in two peaks centred at 941.3 ± 0.6 eV and 943.3 ± 0.6 eV. The analysis of the shape of the obtained spectra and the position of the peaks showed that the distribution of the copper species depended on the nature of the support. For instance, the CuAl-MG catalysts had a main peak centred at 934.4 ± 0.3 eV with two shake-up satellites at 7.1 ± 0.1 and 9.4 ± 0.3 eV higher in binding energy (close to 7.6 and 10 eV which associated with bulk CuO). Nevertheless, the CuAl-P main peaks were situated at 934 ± 0.5 eV with shake-up satellites at 6.5 ± 0.5 and 8.9 ± 0.2 eV higher in BE. Moreover, a significant enrichment of surface copper was observed with increasing Cu loading on the CuAl-MG microstructured catalysts. Indeed, as deduced from Table 4, on the CuAl-MG microstructured catalysts the Cu/Al XPS atomic ratio increased from 0.13 to 0.54, while passing from 8.4 to 14.6 wt% of loaded Cu. However, this ratio seemed to be lower and almost constant (0.07–0.09) on the CuAl-P powder catalysts. The obtained results were in good agreement with the H_2-TPR data where it was concluded that, in contrast to the CuAl-P catalysts, the CuAl-MG catalysts contained a fraction of CuO which did not interact with alumina. Note that despite of the fact that the occurrence of the small fraction of Cu_2O phase was detected for the CuAl-P samples by H_2-TPR, its XPS spectra did not reveal the presence of this species.

The different broadness of the main Cu $2p_{3/2}$ peaks for the examined catalysts and that of CuO reference sample should also be noticed. As revealed by the FWHM data reported in Table 4, the supported copper samples showed much broader peaks, thus suggesting a larger heterogeneity in copper environments. As shown in Fig. 7 the deconvoluted spectra consisted of two peaks with BE of 933.5 ± 0.6 eV and 935 ± 0.6 eV assigned to Cu^{2+} octahedrally and tetrahedrally coordinated, respectively [41]. The occurrence of these copper coordination was very consistent with the UV-visible-NIR results discussed above.

3.8. Catalytic activity in CO oxidation

The CO oxidation reaction was carried out on the CuAl-MG and CuAl-P catalysts. The performance reproducibility of the assayed catalysts was conducted by carrying out a second catalytic run on the catalysts submitted to the same pre-treatment routine realised on the fresh catalysts (heating at 360 °C, in a 20%O_2/He flow, followed by 1 h at 360 °C).

Fig. 8 shows the light-off curves, in CO oxidation reaction, over the CuAl-MG and CuAl-P catalysts. Likewise, Table 5 summarises the obtained results. In addition to the temperature required for 50% (T_{50}) and 90% (T_{90}) CO conversion, the table also shows catalytic activity data at 185 °C and the values of the apparent activation energy calculated in the 150–185 °C range. At these temperatures (CO conversion < 20%) mass transport resistances could be excluded [42]. By using the data reported in Table 4, turnover frequencies (TOF) were estimated. In this estimate, data determined by taking into account the total copper amount (TOF_{TotCu}) and that corresponding to the surface copper exclusively (TOF_{SurfCu}) have been considered.

On the CuAl-MG1 catalyst the activity started around 150 °C. Its conversion increased rapidly to reach 100% at about 270 °C, and remained constant up to 360 °C. On the CuAl-P1 catalyst the CO conversion begins at approximately 140 °C but it did not reach 100% before 340 °C. A second catalytic run, performed on the same catalysts revealed a decrease of the temperature of CO activation on CuAl-MG1 catalyst. The conversion started around 125 °C and increased less abruptly than in the first run. Moreover, the T_{50} (defined as the temperature required for 50% CO conversion) was lower by at least 33 °C from the first to second catalytic run (Table 5). However on the CuAl-P1 powder catalyst the catalytic activity did not undergo any noticeable improvement. In the same way, compared to CuAl-MG1 sample, the catalytic activity of the CuAl-MG2 and CuAl-MG3 catalysts seemed to be improved in the second catalytic run. The latter also became, comparing their T_{50} and T_{90}, more active than their CuAl-P2 and CuAl-P3 counterpart. For instance, on

Table 5
Catalytic activity of CuAl-MG and CuAl-P catalysts in CO oxidation reaction.

Catalysts	Catalytic run	T_{50} (°C)*	T_{90} (°C)*	TOF_{TotCu}[a]·($\times 10^{-4}$ s^{-1})	TOF_{SurfCu}[b]·($\times 10^{-4}$ s^{-1})	E_a (kJ mol^{-1})[c]
CuAl-MG1	1st run	250	271	2.8	3.6	95.3
	2nd run	217	254	11.2	14.8	85.2
CuAl-MG2	1st run	250	288	3.2	5.6	92.5
	2nd run	242	283	4.2	7.6	155
CuAl-MG3	1st run	236	271	3.8	10.2	52.4
	2nd run	226	265	6.4	17.6	60.6
CuAl-P1	1st run	247	292	5.4	12.2	43.0
	2nd run	248	292	5.4	12.2	46.6
CuAl-P2	1st run	254	304	3.4	13	43.3
	2nd run	256	299	3.4	13	42.1
CuAl-P3	1st run	247	291	3.8	28	40.8
	2nd run	250	294	3.8	28	25.8
Cu-MG	1st run	338	410	0.4	–	8500
	2nd run	338	405	0.4	–	8500

[a] Turnover frequency referred to 1 mol of total copper (calculated at 185 °C).
[b] Turnover frequency referred to 1 mol of surface copper (calculated at 185 °C).
[c] Activation energy determined in 150–185 °C range.
(*) Defined as the temperature required for 50% and 90% CO conversion.

CuAl-MG3 the activity reached 90% at 265 °C whereas over CuAl-P3 a temperature equal to 294 °C was required. Additionally, the morphology and the general aspect of the tested CuAl-MG microreactors were examined by SEM. Their micrographs did not show any noticeable difference when compared with that of the fresh samples. Moreover, no significant weight loss was noticed after the two catalytic runs.

The improvement of the catalytic activity, in the second catalytic run, of the CuAl-MG catalysts was due probably to the activation caused by a re-dispersion of the Cu species. As mentioned above, our characterisation results showed that three types of copper species were detected in the series of the CuAl-MG microstructured catalysts: (i) CuO deposited on the surface of the substrate (restricted to Cu/Al molar ratios superior to 0.07); (ii) highly dispersed CuO on the alumina and (iii) bulk CuO. By contrast, on the CuAl-P powdered catalysts the highly dispersed CuO on the alumina support together with small amount of Cu_2O species were detected. To confirm the re-dispersion phenomenon of the copper species on the CuAl-MG catalysts H_2-TPR experiment was carried out on the samples extracted after the first catalytic run (with reoxidation at 400 °C). Only the results obtained with the CuAl-MG1 microstructured catalyst were reported here because they were the most significant (Fig. 9). As reported in Fig. 9 the H_2-TPR profile of the tested CuAl-MG1 showed that, in contrast to the H_2-TPR trace of the fresh one (also displayed in Fig. 4 where it was composed of two reduction peaks at 215 and 270 °C), it was composed by three distinct reducible species of copper. The presence of an additional reduction peak situated at 330 °C, attributed to the fraction of CuO interacting with the substrate surface, could explain the improvement of the catalytic activity of the CuAl-MG1 catalyst in its second catalytic run. In order to probe the activity of the fraction of CuO interacting with the substrate in CO oxidation similar experiment was carried out on the Cu-MG sample. As shown in Table 5, the latter had very low activity compared to all the assayed catalysts (T_{50} = 338 °C, T_{90} = 410 °C). The obtained results excluded the high activity of the fraction of CuO interacting with the substrate. However, since the temperature could influence the light-off behaviour in the CO oxidation reaction, the thermal conductivity was another factor to take into consideration in order to explain the different performances of the CuAl-MG and CuAl-P catalysts in CO oxidation reaction. Since cupric oxide has very high thermal conductivity (78 W m^{-1} K^{-1} [43]), compared to alumina (40 W m^{-1} K^{-1}), we thought that the fraction of CuO deposited on the substrate and presenting low heat transfer resistance could easily dissipate the heat generated in the Cu/Al_2O_3 film by the exothermic CO oxidation reaction or by the re-oxidation of the Cu species and increased homogeneously the catalyst bed temperature. Accordingly, in their study on the behaviour of copper and copper oxides in CO oxidation reaction, Huang et al. [22] claimed that the CO oxidation should release heat of reaction and increase the catalyst bed temperature and, thus, the high CO oxidation activity and the high bed temperature are maintained simultaneously.

It should be noted that a careful analysis of the resulting TOF data, calculated at 185 °C (Table 5), showed a significant difference compared to the observation presented above. Obviously, the TOF values referred to the total copper (TOF_{TotCu}) were always smaller than those referred to the surface copper (TOF_{SurfCu}) for the same catalyst. In the first catalytic run, TOF_{TotCu} values were ranging from 2.8×10^{-4} to 3.8×10^{-4} s^{-1} on the series of the CuAl-MG microreactors while over the CuAl-P catalysts they were in the 3.4×10^{-4}–5.4×10^{-4} s^{-1} range. However, in the second catalytic run, the CuAl-MG catalysts had higher TOF_{TotCu} values (4.2×10^{-4}–11.2×10^{-4} s^{-1}) compared to their counterpart in powder (3.4×10^{-4}–5.4×10^{-4} s^{-1}). For instance, the calculated TOF_{TotCu} was twice on the CuAl-MG1 microreactor (11.2×10^{-4} s^{-1}) than on the CuAl-P1 powder catalyst (5.4×10^{-4} s^{-1}).

On the other hand, the TOF_{SurfCu}, referred to 1 mol of surface copper, on the CuAl-P powder catalysts increased with copper loading and approached 2.8×10^{-4} s^{-1} on CuAl-P3 (Table 5); but it stayed almost constant after the second catalytic run compared to the first one. It should be noted that the CuAl-MG microreactors showed a different behaviour. Indeed, the TOF_{SurfCu} increased significantly in the second catalytic run suggesting their apparent activation. Moreover, the CuAl-MG3 became the most active microreactor in the first ($TOF_{SurfCu} = 10.2 \times 10^{-4}$ s^{-1}) and the second catalytic run ($TOF_{SurfCu} = 17.6 \times 10^{-4}$ s^{-1}). However, these values were significantly lower when compared with its counterpart in powder shape (CuAl-P3). Likewise, the activation energy was in all the cases lower on the CuAl-P powder catalysts (25–46 kJ.mol^{-1}) compared to the CuAl-MG reactors (52–155 kJ mol^{-1}). The difference between the two series of the assayed catalysts was probably related to the active copper species laying on the surface. The greater activity of the CuAl-P catalysts at low temperatures <190 °C, suggested that they possessed more efficient copper sites than CuAl-MG catalysts. Effectively, in accordance with our H_2-TPR results we concluded that the catalysts which contained Cu_2O species (CuAl-P), which

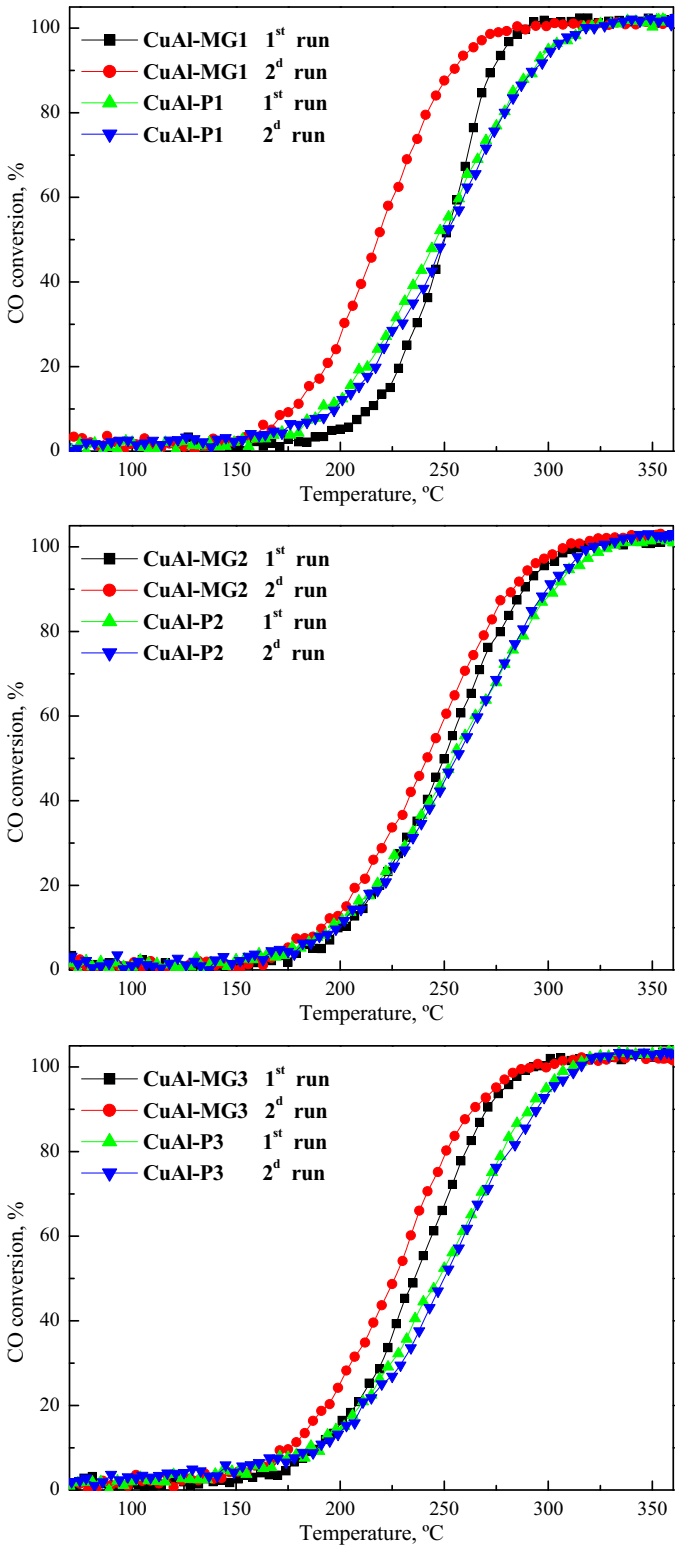

Fig. 8. CO conversion in CO oxidation reaction over CuAl-MG and CuAl-P catalysts vs. the reaction temperature.

were assumed to be involved in the CO oxidation reaction, were more active, at low temperatures, than the CuAl-MG catalysts. This proposal was in good agreement with earlier studies [22,23], in accordance with which, in CO oxidation reaction, the Cu_2O is the most active Cu species at low temperatures (<200 °C).

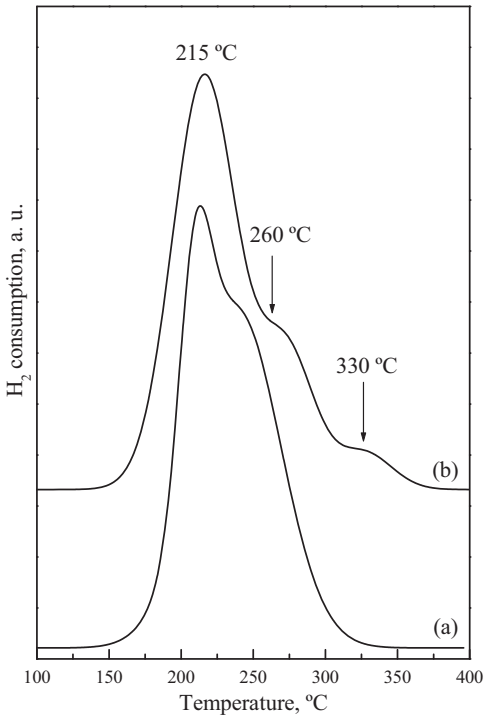

Fig. 9. H_2-TPR profiles of (a) CuAl-MG1 and (b) CuAl-MG1 after CO oxidation catalytic test.

4. Conclusions

Homogeneous and well adhered alumina washcoats were synthesised onto stainless steel microgrids. The resulted microreactors were impregnated with copper oxide (with three different Cu/Al molar ratios), characterised by SEM, BET, XRD, H_2-TPR, UV-Visible NIR and XPS and tested in CO oxidation reaction. For comparison, preparation, characterisation and catalytic run were also taken on a series of the powdered catalysts with the same Cu/Al atomic ratios.

H_2-TPR, UV-Visible-NIR and XPS analyses showed that CuO existed in three forms in the prepared microreactors: (i) CuO deposited on the surface of the substrate, (ii) highly dispersed CuO on the alumina surface and (iii) bulk CuO. However, the highly dispersed CuO on the alumina support together with small amount of Cu_2O species were detected in the Cu/Al_2O_3 powdered catalysts.

In the CO oxidation reaction, the CuAl-P powder catalysts seemed to be more active at low temperatures (<200 °C) due to the high activity of their Cu_2O species. However, at high temperatures, when activated under reaction gas mixture, the CuAl-MG microstructured catalysts were more active than the CuAl-P powdered catalysts (with the same Cu/Al molar ratio). The copper distribution in the microstructured catalysts seemed to play a decisive role in their activity. Indeed, the H_2-TPR analysis of the most active catalyst after catalytic test showed a beneficent redistribution of the copper in the microreactor during the CO oxidation reaction. This was explained by the generation of CuO interacting with the substrate and presenting low heat transfer resistance which could easily dissipate the heat generated, in the Cu/Al_2O_3 film, by the exothermic CO oxidation reaction or by the re-oxidation of the Cu species and increased homogeneously the catalyst bed temperature.

These catalytic features evidenced the potential of CuAl-MG as a promising alternative catalyst in the CO oxidation reaction.

Acknowledgements

The financial support for this work provided by Gobierno Vasco (GIC IT-657-13) and UPV/EHU (UFI11/39) is gratefully acknowledged.

References

[1] G. Kolb, V. Hessel, Chem. Eng. J. 98 (2004) 1–38.
[2] L. Kiwi-Minsker, A. Renken, Catal. Today 110 (2005) 2–14.
[3] R.S. Besser, X. Quyang, H. Surangalikar, Chem. Eng. Sci. 58 (2003) 19–26.
[4] H. Surangalikar, X. Quyang, R.S. Besser, Chem. Eng. J. 93 (2003) 217–224.
[5] I. Yuranov, A. Renken, L. Kiwi-Minsker, Appl. Catal. A 281 (2005) 55–60.
[6] S.K. Ajmera, C. Delattre, M.A. Schmidt, K.F. Jensen, J. Catal. 209 (2002) 401–412.
[7] N.R. Peela, A. Mubayi, D. Kunzru, Catal. Today 147S (2009) S17–S23.
[8] M. Valentini, G. Groppi, C. Cristiani, M. Levi, E. Tronconi, P. Forzatti, Catal. Today 69 (2001) 307–314.
[9] A. Stefanescu, A.C. van Veen, E. Duval-Brunel, C. Mirodatos, Chem. Eng. Sci. 62 (2007) 5092–5096.
[10] A. Stefanescu, A.C. van Veen, C. Mirodatos, J.C. Beziat, E. Duval-Brunel, Catal. Today 125 (2007) 16–23.
[11] G. Park, S. Yim, Y. Yoon, W. Lee, C. Kim, D. Seo, K. Eguchi, J. Power Sources 145 (2005) 702–706.
[12] I. Aartun, T. Gjervan, H. Venvik, O. Görke, P. Pfeifer, M. Fathi, A. Holmen, K. Schubert, Chem. Eng. J. 101 (2004) 93–99.
[13] K. Haas-Santo, O. Görke, P. Pfeifer, K. Schubert, Chimia 56 (11) (2002) 605–610.
[14] G. Germani, A. Stefanescu, Y. Schurmann, A.C. Veen, Chem. Eng. Sci. 62 (2007) 5084–5091.
[15] B. Monnerat, L. Kiwi-Minsker, A. Renken, Chem. Eng. Sci. 56 (2001) 633–639.
[16] I. Yuranov, N. Dunand, L. Kiwi-Minsker, Appl. Catal. B 36 (2002) 183–191.
[17] G. Marban, I. López, T. Valdés-Solis, A.B. Fuertes, Int. J. Hydrogen Energ. 33 (2008) 6687–6695.
[18] N.C. Pérez, E.E. Miró, J.M. Zamaro, Appl. Catal. B 129 (2013) 416–425.
[19] C. Li, R. Lin, H. Lin, Y. Lin, K. Chen, Chem. Commun. 47 (2011) 1473–1475.
[20] M. Luo, P. Fang, M. He, Y. Xie, J. Mol. Catal. A 239 (2005) 243–248.
[21] P.W. Park, J.S. Ledford, Appl. Catal. B 15 (1998) 221–231.
[22] T. Huang, D. Tsai, Catal. Lett. 87 (2003) 173–178.
[23] H. Wan, Z. Wang, J. Zhu, X. Li, B. Liu, F. Gao, L. Dong, Y. Chen, Appl. Catal. B 79 (2008) 254–261.
[24] L. Villegas, F. Masset, N. Guilhaume, Appl. Catal. A 320 (2007) 43–55.
[25] A. Eleta, P. Navarro, L. Costa, M. Montes, Micropor. Mesopor. Mat. 123 (2009) 113–122.
[26] P. Avila, M. Montes, E.E. Miró, Chem. Eng. J. 109 (2005) 11–36.
[27] V. Meille, S. Pallier, G.V.S.C. Bustamante, M. Roumanie, J.P. Reymond, Appl. Catal. A 286 (2005) 232–238.
[28] F.E. López-Suárez, A. Bueno-López, M.J. Illán-Gómez, Appl. Catal. B 84 (2008) 651–658.
[29] A. Gervasini, S. Bennici, Appl. Catal. A 281 (2005) 199–205.
[30] M. Sun, X. Wu, Z. Zhang, E. Han, Corros. Sci. 51 (2009) 1069–1072.
[31] T. shyr, J. Shie, S. Huang, W. Hwang, Mater. Chem. Phys. 122 (2010) 273–277.
[32] H. Mai, L. Mengfei, F. Ping, J. Rare Earth 24 (2006) 188–192.
[33] C. Chen, W. Cheng, S. Lin, Catal. Lett. 68 (2000) 45–48.
[34] M.L. Jacono, A. Cimino, M. Inversi, J. Catal. 76 (1982) 320–332.
[35] R. Hierl, H. Zinger, H.P. Urbach, J. Catal. 69 (1981) 475–486.
[36] J.J. Bravo-Suárez, B. Subramaniam, R.V. Chaudhari, J. Phys. Chem. C 116 (2012) 18207–18221.
[37] R.A. Schoonheydt, Catal. Rev.: Sci. Eng. 35 (1993) 129–168.
[38] M. Iwamoto, H. Yahiro, N. Mizuno, W.X. Zhang, Y. Mine, H. Furukawa, S. Kagawa, J. Phys. Chem. 96 (1992) 9360–9366.
[39] J.F. Xu, W. Ji, Z.X. Shen, S.H. Tang, X.R. Ye, D.Z. Jia, X.Q. Xin, J. Solid State Chem. 147 (1999) 516–519.
[40] J.P. Espinos, J. Morales, A. Barranco, A. Caballero, J.P. Holgado, A.R. González-Elipe, J. Phys. Chem. B 106 (2002) 6921–6929.
[41] Z. Xiao, J. Xiu, X. Wang, B. Zhang, C.T. Williams, D. Su, C. Liang, Catal. Sci. Technol. 3 (2013) 1108–1115.
[42] M.J. Kahlich, H.A. Gasteiger, R.J. Behm, J. Catal. 171 (1997) 93–105.
[43] D. Anandan, K.S. Rajan, Asian J. Sci. Res. 5 (2012) 218–227.